Supplementary Document

Ensemble Number	ENS1	ENS2	ENS3	ENS4	ENS5	ENS6	ENS7	ENS8	ENS9
ENSO (DJF)	Warm	Cold	Cold	Warm	Cold	Neutral	Cold	Neutral	Warm
QBO (@30hPa)	Easterly	Easterly	Easterly	Easterly	Westerly	Easterly	Easterly	Westerly	Westerly
Ensemble Number	ENS10	ENS11	ENS12	ENS13	ENS14	ENS15	ENS16	ENS17	ENS18
ENSO (DJF)	Warm	Cold	Cold	Warm	Cold	Neutral	Cold	Neutral	Warm
QBO (@30hPa)	Easterly	Easterly	Easterly	Easterly	Westerly	Westerly	Easterly	Westerly	Westerly

Table S1. UKESM Ensemble Season, QBO, and ENSO Initial Phase Classifications.

Additional Explanation of QBO and ENSO Classifications

The QBO is a downward propagating quasiperiodic oscillation of the equatorial zonal wind between easterlies and westerlies in the tropical stratosphere (Baldwin et al., 2001). In this study QBO state was characterized by the wind velocity between 15°N and 15°S, across all longitudes at a pressure of 30hPa, with initial QBO state being defined at the month of eruption. Positive wind velocities denote a Westerly QBO phase with negative ones denoting an Easterly phase. This resulted in 6 easterly and 3 westerly classified July ensembles and 5 easterly and 4 westerly classified January ensembles.

The ENSO is an interannual climate variation, characterized by a cycle of anomalous winds and sea surface temperatures (SST) over the tropical eastern Pacific. The warm SST phase, coupled with weakened trade winds, is known as El Niño and the cold phase, accompanied by enhanced trade winds, as La Niña, with a neutral phase in between. In this study ENSO phase was characterized as either warm, cold, or neutral using the December-January-February (DJF) NH Winter Niño 3.4 Index, where January is the reference for the year, as done by Zanchettin et al., (2016). To classify the ensembles the spatially averaged mean DJF SST anomaly was calculated for the Niño 3.4 region (5°N-5°S, 170°W-120°W) with warm and cold phases defined when the anomalies exceed +/- 0.4°C respectively (Trenberth and Stepaniak, 2001). This resulted in 3 warm, 2 neutral, and 4 cold phase classified ensembles across both January and July ensembles.

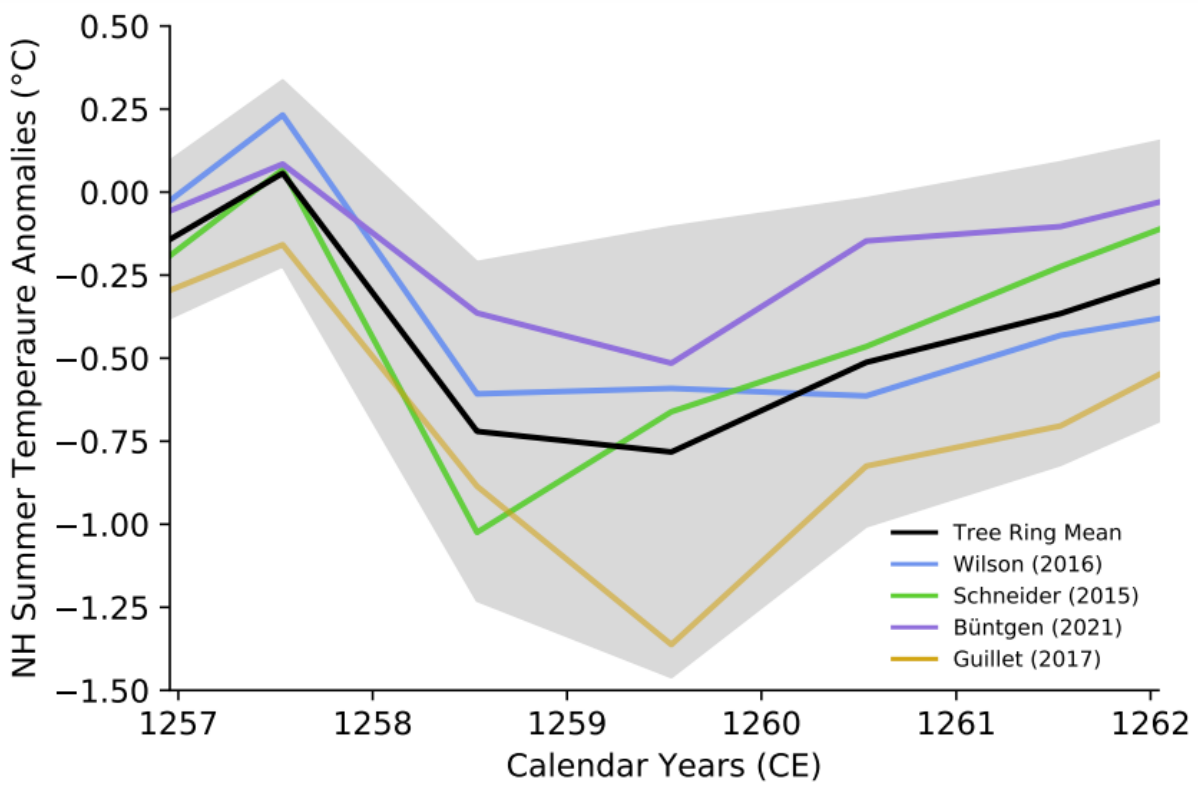

Figure S1. Northern Hemisphere Summer (June-July-August) Temperature Anomalies for Individual Tree Ring Reconstruction datasets. Black line shows the tree-ring reconstructed mean utilised in the main text Figure 1 with the grey band showing 2σ around the mean.

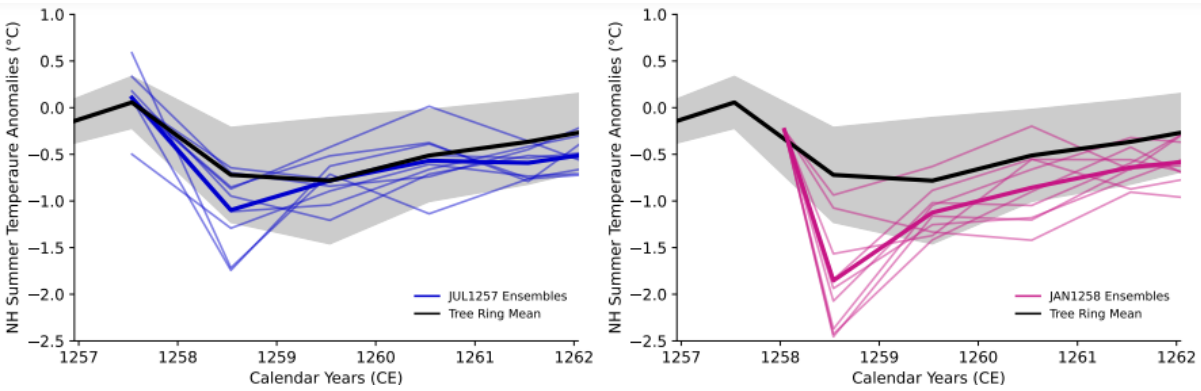

Figure S2. Model-simulated Northern Hemisphere Summer (June-July-August) Temperature Anomalies for individual July 1257 (left) and January 1258 (right) ensembles. Black line shows the tree-ring reconstructed mean with the grey band showing 2σ around the mean. Thin lines show individual ensembles, and the thick line shows the model-simulated ensemble mean. Of the 9 July 1257 ensembles 6 lie within 2σ of the tree ring-reconstructed mean for Summer 1258 whereas for the January 1258 ensembles only 2 lie within 2σ of the tree ring-reconstructed mean for Summer 1258.

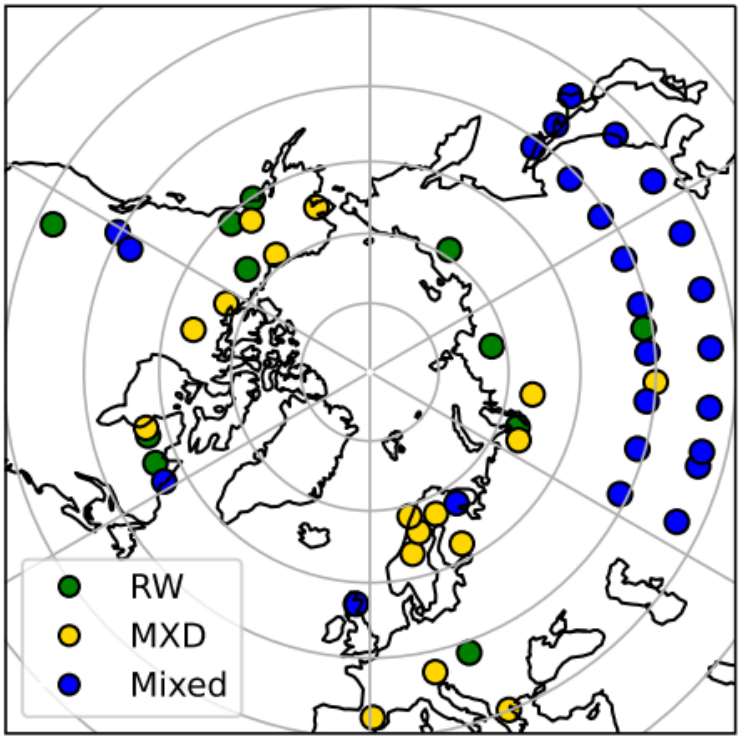

Figure S3: Spatial distribution of sites used in the NTREND reconstruction, with proxy type shown by colour. NTREND data from Wilson et al., (2016) and Anchukaitis et al., (2017) , plot after Fig 1 in Wilson et al., (2016).

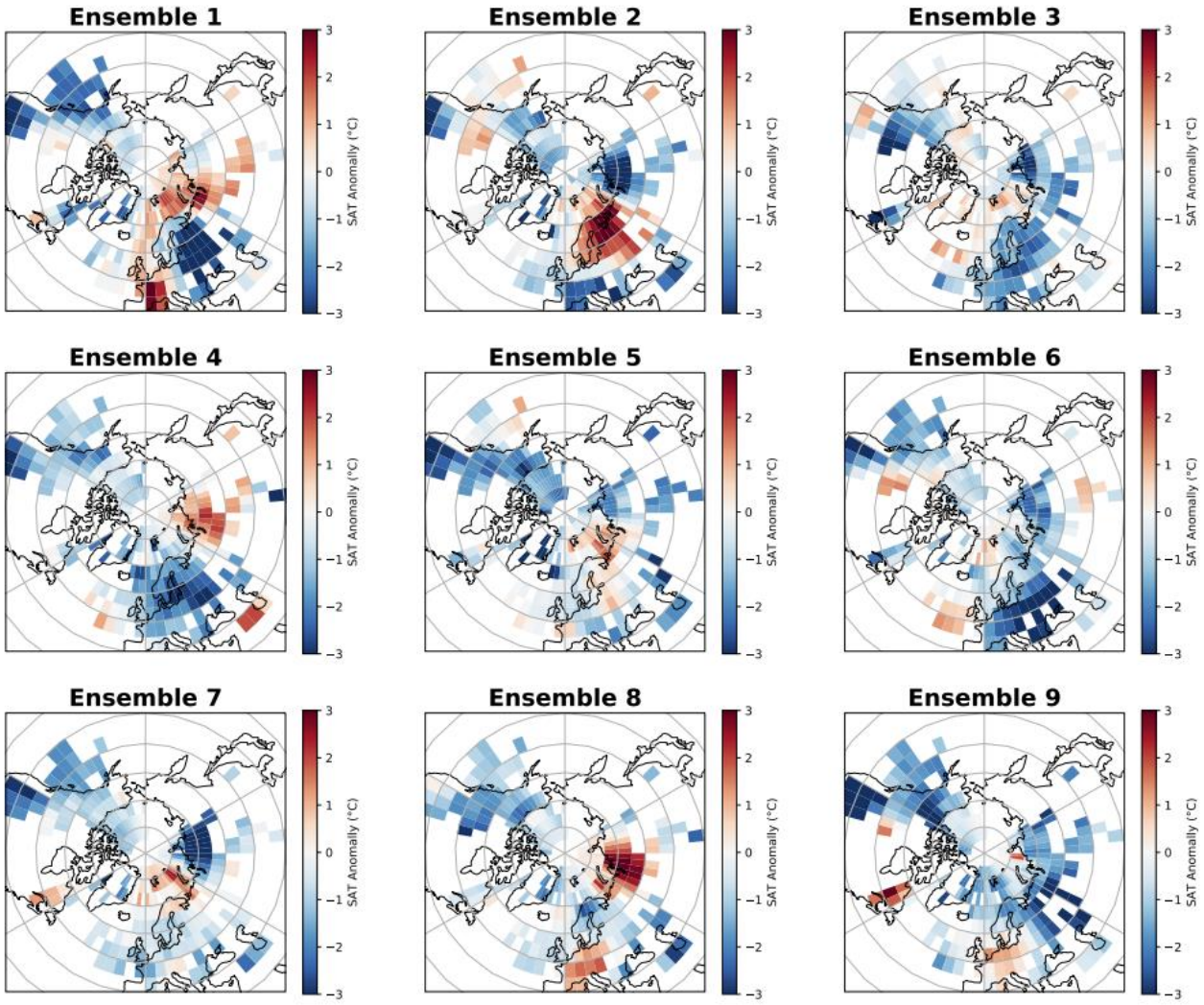

Figure S4. Spatially resolved NH Summer (JJA) Temperature Anomalies for individual JUL1257 ensembles for Summer 1258. Model-simulated anomalies were regridded to be comparable to the NTREND spatially resolved dataset (Anchukaitis et al., 2017).

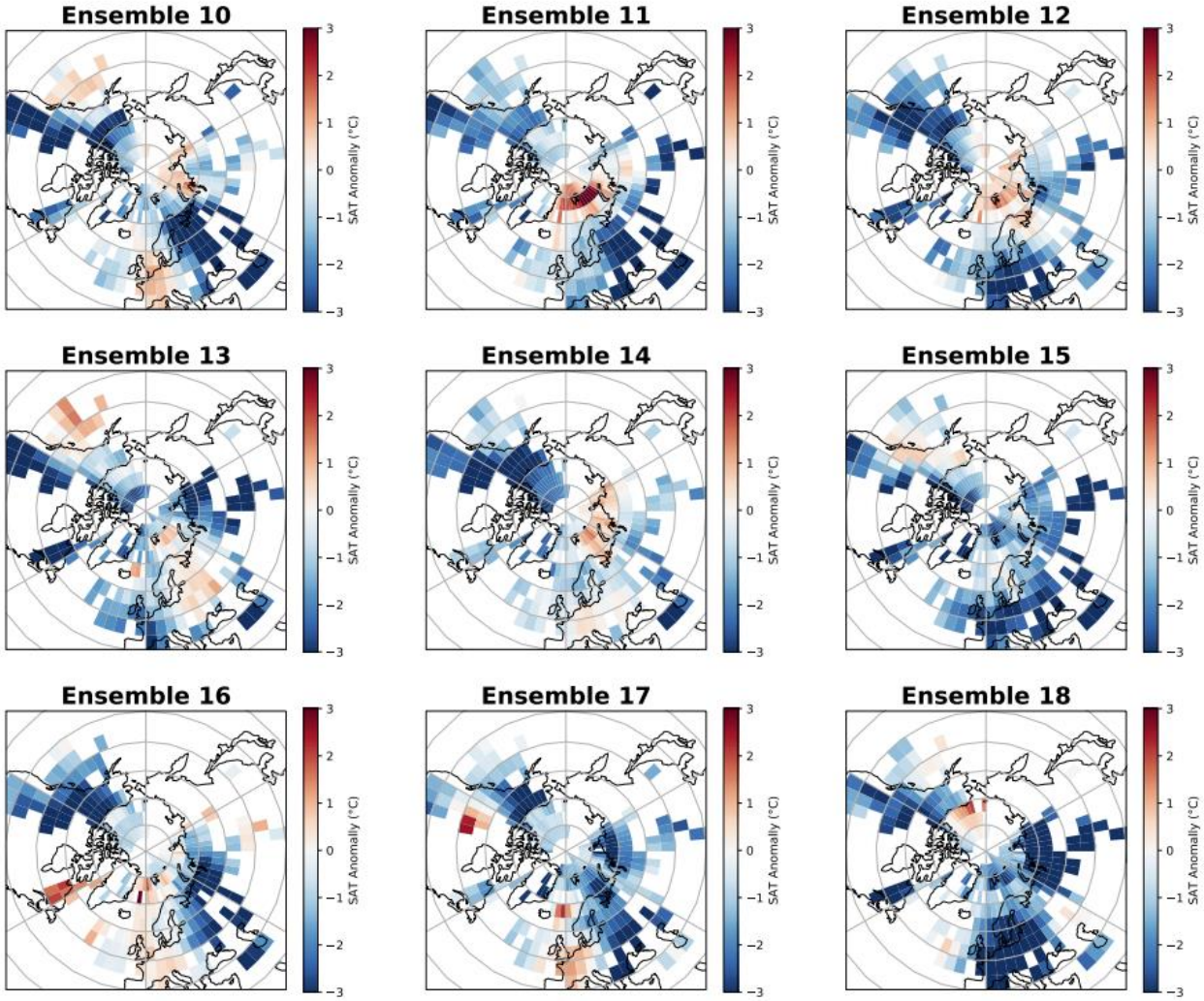

Figure S5. Spatially resolved NH Summer (JJA) Temperature Anomalies for individual JAN1258 ensembles for Summer 1258. Model-simulated anomalies were regridded to be comparable to the NTREND spatially resolved dataset (Anchukaitis et al., 2017).

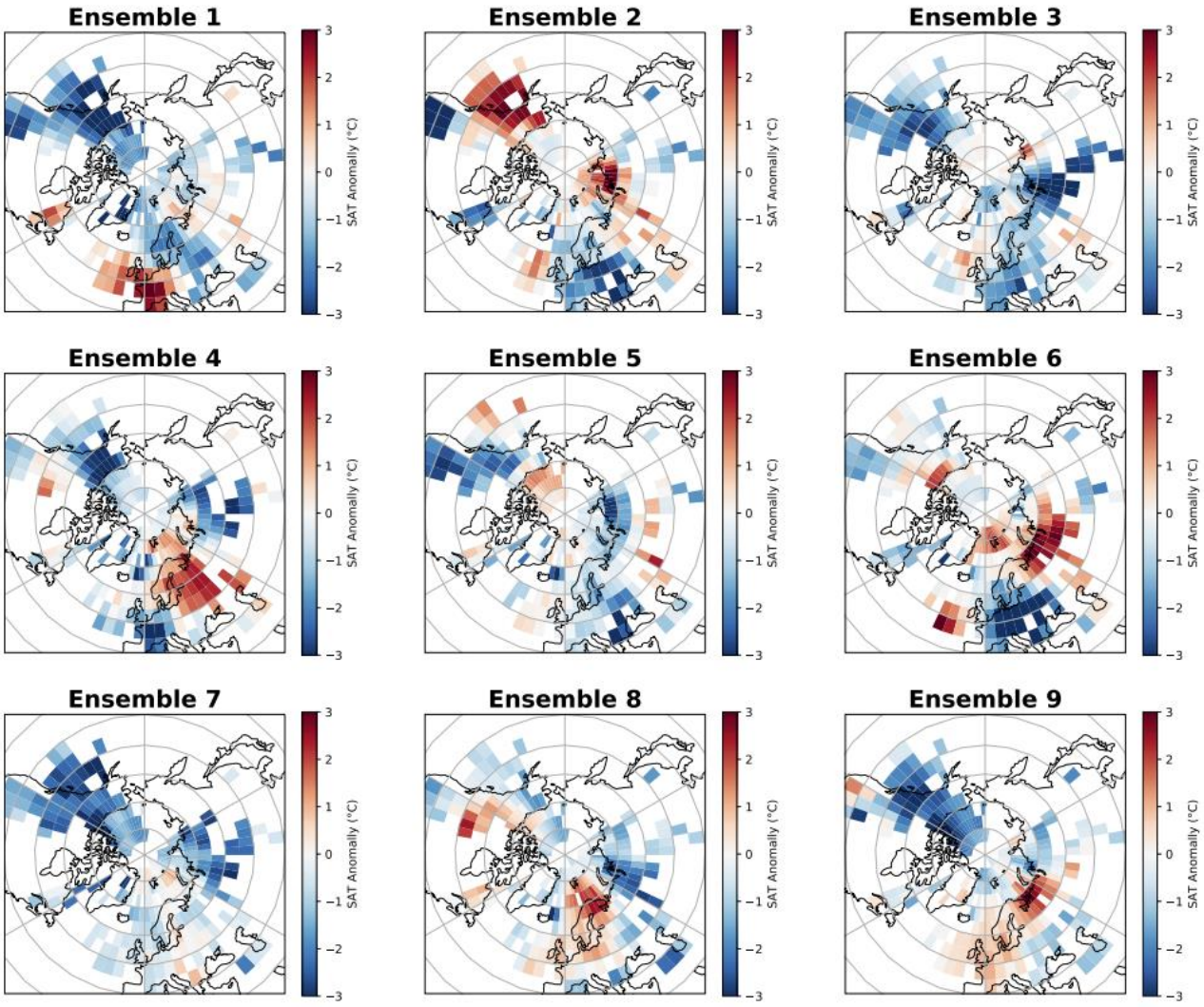

Figure S6. Spatially resolved NH Summer (JJA) Temperature Anomalies for individual JUL1257 ensembles for Summer 1259. Model-simulated anomalies were regridded to be comparable to the NTREND spatially resolved dataset (Anchukaitis et al., 2017).

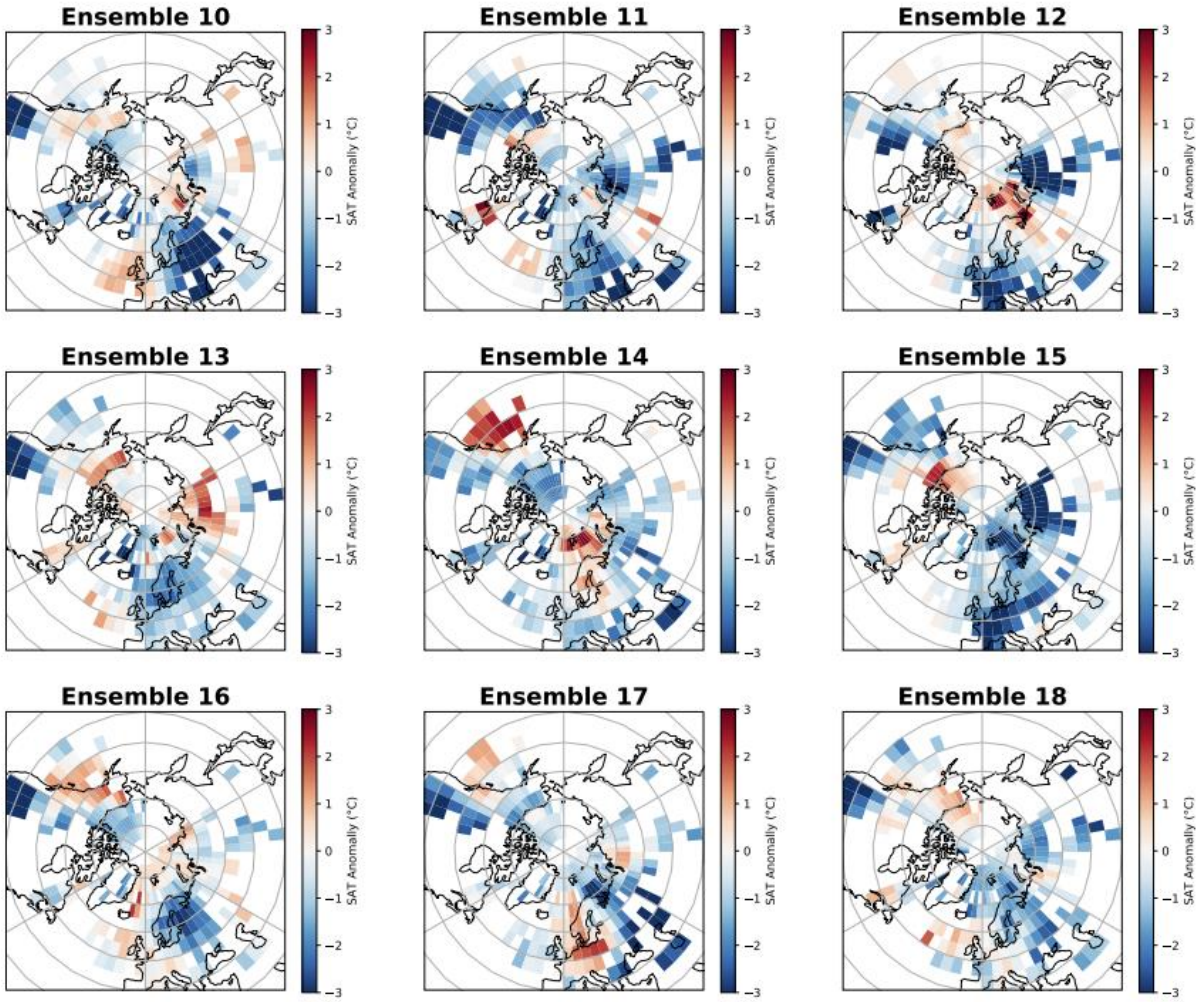

Figure S7. Spatially resolved NH Summer (JJA) Temperature Anomalies for individual JAN1258 ensembles for Summer 1259. Model-simulated anomalies were regridded to be comparable to the NTREND spatially resolved dataset (Anchukaitis et al., 2017).

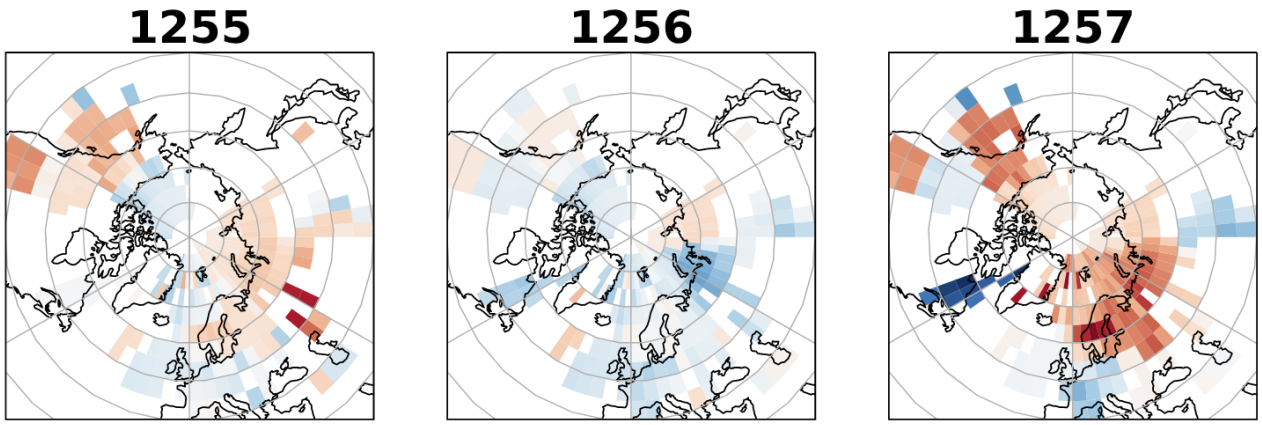

Figure S8. NTREND NH Summer (JJA) Tree Ring-reconstructed SAT reconstructions 1255-1257 (Anchukaitis et al., 2017). Moderate positive SAT anomalies are present in Alaska and the US West Coast in 1255 with the onset of strong positive SAT anomalies occurring in 1257. This may be indicative of prevailing warm phase El Nino-like conditions in 1257 prior to the Mt Samalas Eruption.

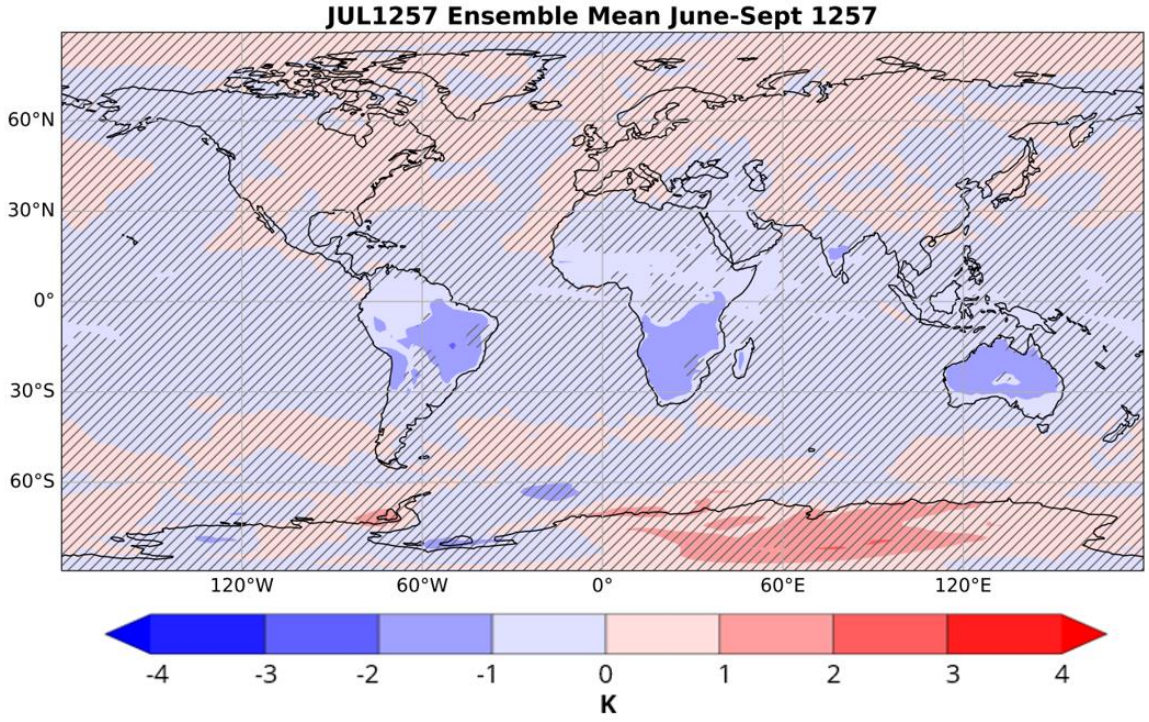

Figure S9: Model-simulated surface air temperature anomalies averaged for June-Sept 1257 for a JUL1257 eruption. Hashed lines denote regions of < 95% significance as determined by a grid point ANOVA test. Only Significant negative anomalies are only seen over the continents in the Southern Hemisphere of up to -2°C. No negative anomalies occur at >95% significance along the West Coast of the US or Canada.

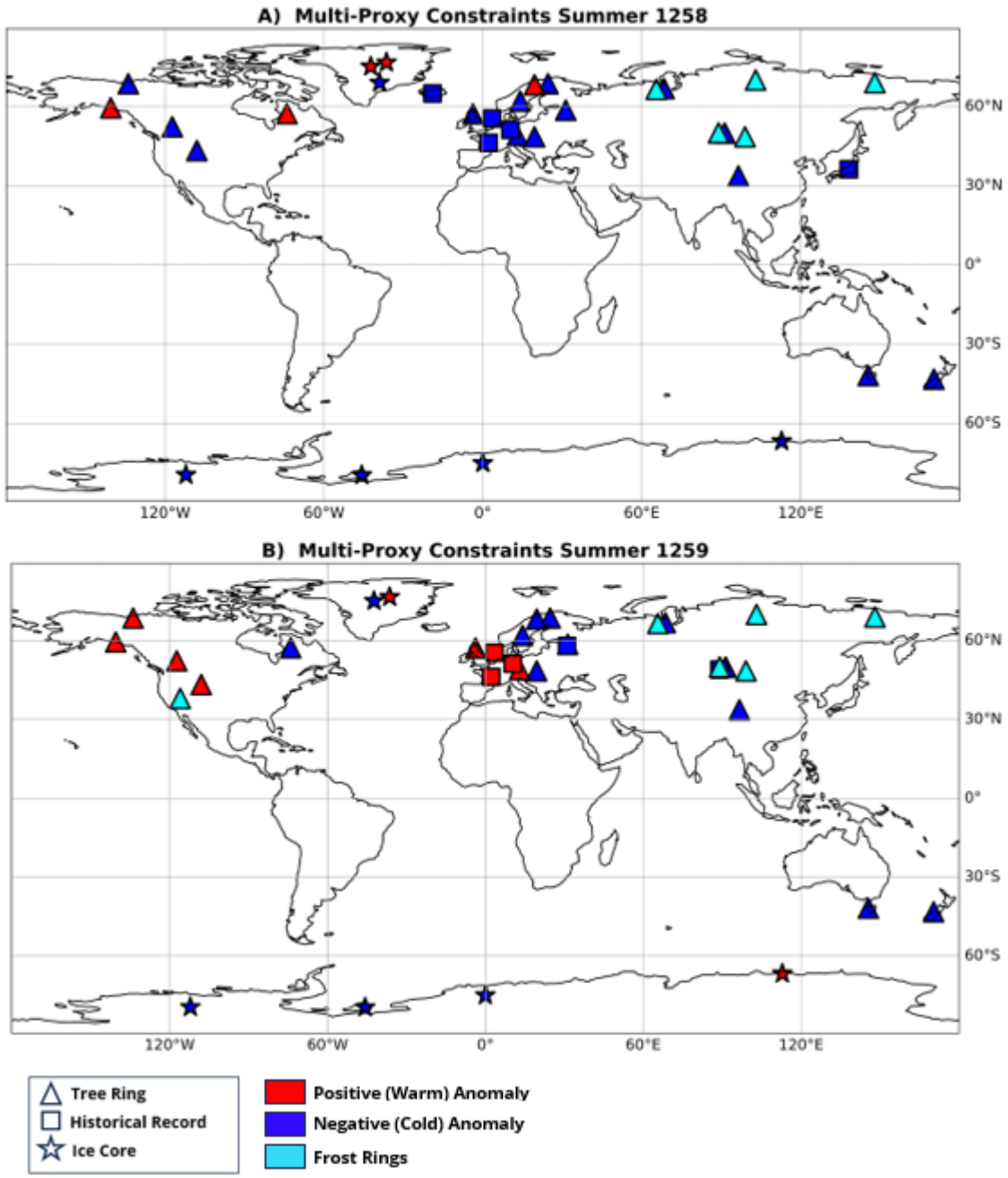

Figure S10: Map showing the locations of records included in the multi-proxy database for summer 1258 and 1259. Red/Blue colouring shows positive or negative SAT anomalies respectively, where light blue shading specifically refers to frost rings (i.e non-quantitative tree ring records). Historical records (square symbol) may only make reference to abnormal weather conditions in one year and therefore may only be present on one panel.

Ice Core Record	SO_4 Rise	SO_4 Peak
Greenland		
NEEM (Sigl et al., 2013)	1258.2	1259.0
NGRIP (Plummer et al., 2012)	1258.1	1259.4
Average:	1258.15 (1258 - February)	1259.2 (1259 - March)
Antarctica		
WDC06A (Sigl et al., 2013)	1257.9	1258.9
Law Dome (Plummer et al., 2012, Jong et al., 2022)	1257.4	1258.3
Average:	1257.65 (1257 – August)	1258.6 (1258 - July)
Average Timing Offset	+ 6 months	+ 8 months
Total Deposition		
Sulfate Antarctica (Kg km-2) (Toohey & Sigl 2017)	73	
Greenland Deposition (Kg km-2)	105	
Greenland/Antarctica	1.4	

Table S2: Ice core records of polar sulfate deposition following the Samalas 1257 eruption

Model	Mean Antarctica deposited sulfate (kg SO4 km-2)	Mean Greenland deposited sulfate (kg SO4 km-2)	Antarctica/Greenland deposition ratio
CESM1(WACCM)	36	109	0.3
MAECHAM5-HAM	264	194	1.4
SOCOL-AER	163	148	1.1
UM-UKCA	19	31	0.6

Table S3: Greenland and Antarctica ice sheet ensemble mean cumulative deposited sulfate and ratio (Antarctica deposition / Greenland deposition) and for each model tested by Marshall et al., 2018.

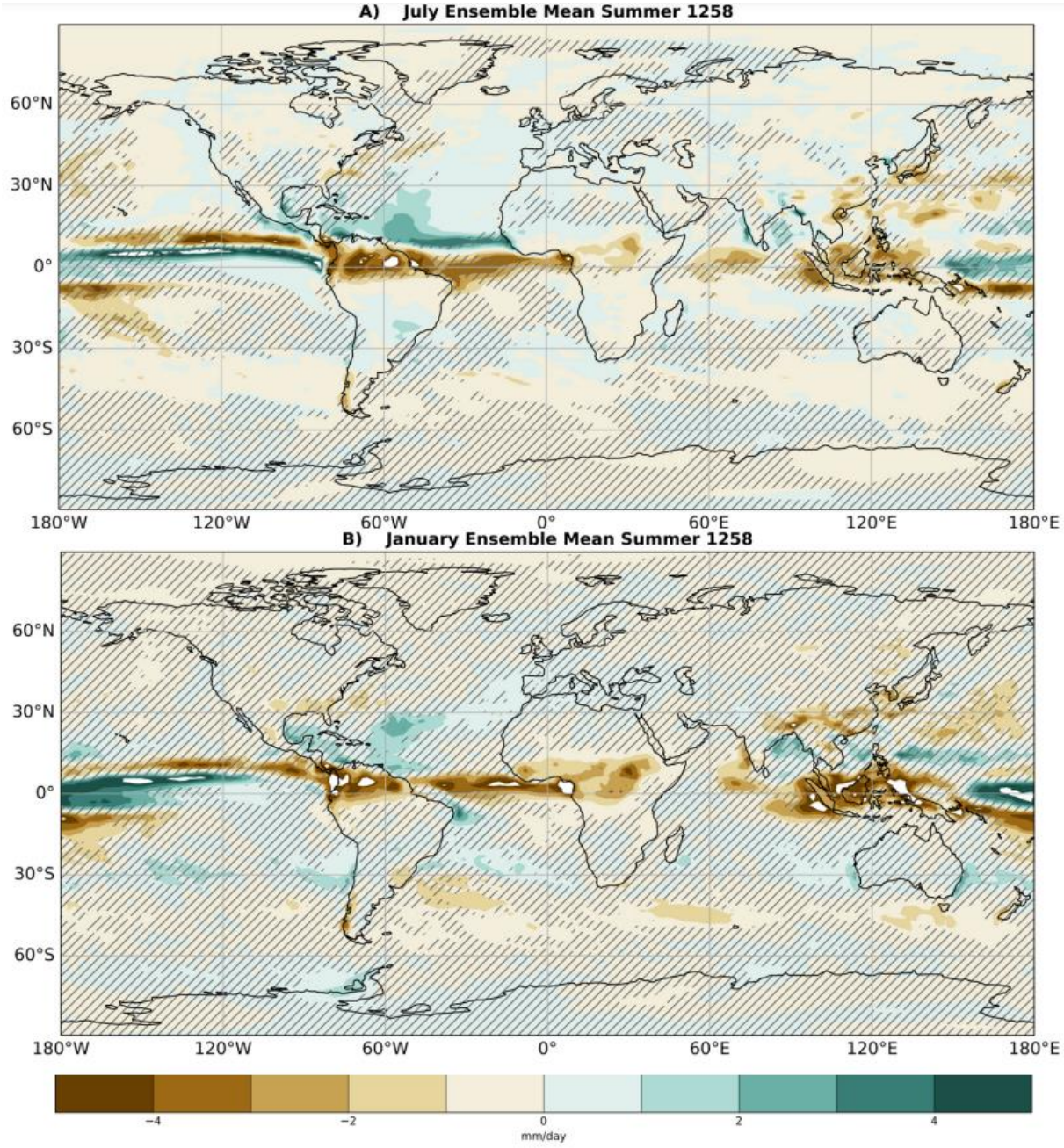

Figure S10. Globally resolved NH Summer (JJA) Precipitation Anomalies for the JUL1257 ensemble mean (Top) and the JAN1258 ensemble mean (Bottom) for Summer 1258. Hashed lines denote anomalies at <95% significance as determined by a grid point ANOVA analysis.